

# Assessing the Viability of $A_4$ , $S_4$ and $A_5$ Flavour Symmetries for Description of Neutrino Mixing

S. T. Petcov<sup>a,b,1</sup> and A. V. Titov<sup>c,2</sup>

<sup>a</sup> *SISSA/INFN, Via Bonomea 265, 34136 Trieste, Italy*

<sup>b</sup> *Kavli IPMU (WPI), University of Tokyo, 5-1-5 Kashiwanoha, 277-8583 Kashiwa, Japan*

<sup>c</sup> *Institute for Particle Physics Phenomenology, Department of Physics, Durham University,  
South Road, Durham DH1 3LE, United Kingdom*

## Abstract

We consider the  $A_4$ ,  $S_4$  and  $A_5$  discrete lepton flavour symmetries in the case of 3-neutrino mixing, broken down to non-trivial residual symmetries in the charged lepton and neutrino sectors in such a way that at least one of them is a  $Z_2$ . Such symmetry breaking patterns lead to predictions for some of the three neutrino mixing angles and/or the leptonic Dirac CP violation phase  $\delta$  of the neutrino mixing matrix. We assess the viability of these predictions by performing a statistical analysis which uses as an input the latest global data on the neutrino mixing parameters. We find 14 phenomenologically viable cases providing distinct predictions for some of the mixing angles and/or the Dirac phase  $\delta$ . Employing the current best fit values of the three neutrino mixing angles, we perform a statistical analysis of these cases taking into account the prospective uncertainties in the determination of the mixing angles, planned to be achieved in currently running (Daya Bay) and the next generation (JUNO, T2HK, DUNE) of neutrino oscillation experiments. We find that only six cases would be compatible with these prospective data. We show that this number is likely to be further reduced by a precision measurement of  $\delta$ .

---

<sup>1</sup>Also at Institute of Nuclear Research and Nuclear Energy, Bulgarian Academy of Sciences, 1784 Sofia, Bulgaria.

<sup>2</sup>E-mail: [arsenii.titov@durham.ac.uk](mailto:arsenii.titov@durham.ac.uk)

# 1 Introduction

Flavour is one of the biggest riddles in particle physics. In spite of the tremendous success of the Standard Theory, yet we do not know why the number of fermion generations is three, what determines the patterns of quark and lepton masses, and what the origins of quark and neutrino mixing are.

Since symmetries proved to be very powerful in guiding the laws of particle physics, it is natural to expect that symmetry might also be a clue to the solution of the flavour problem. For this reason, a variety of *flavour symmetries* have been proposed and explored in the attempts to understand the observed patterns of quark and/or neutrino mixing and of the quark and/or lepton masses. Symmetries described by both continuous groups, including  $U(1)$ ,  $SU(2)$ ,  $U(2)$ ,  $SU(3)$ ,  $U(3)$  (see, e.g., [1–6]), and discrete groups, such as  $S_3$ ,  $S_4$ ,  $A_4$ ,  $T'$ ,  $A_5$ , as well as the series  $D_n$ ,  $\Delta(3n^2)$ ,  $\Delta(6n^2)$  with  $n \in \mathbb{N}$  and  $\Sigma$  groups (see, e.g., [7–9] for reviews and original references) have been considered. Discrete non-Abelian symmetries allow for rotations in the flavour space by fixed (large) angles, which is particularly attractive in view of the fact that two of the three neutrino mixing angles are large [10–12]. Thus, neutrino mixing, as suggested, e.g., in [13], seems to be the appropriate flavour related structure to search for evidence of existence of an underlying flavour symmetry, and therefore for New Physics.

In the framework of discrete flavour symmetry approach to 3-neutrino mixing<sup>1</sup>, on which we will concentrate in the present article, it is assumed that at some high-energy scale there exists a (lepton) flavour symmetry described by a non-Abelian discrete (finite) group. The lepton doublets of the three fermion generations are usually (but not universally) assigned to an irreducible 3-dimensional representation of this group, because one aims to unify the three lepton flavours, and this is the case we will consider in the present article. At low energies the flavour symmetry has necessarily to be broken, because the electron, muon and tauon charged leptons and the three massive neutrinos are distinct. Generally, the flavour symmetry group  $G_f$  is broken in such a way that the charged lepton and neutrino mass matrices,  $M_e$  and  $M_\nu$ <sup>2</sup>, or more precisely, the combination  $M_e M_e^\dagger$  and  $M_\nu (M_\nu^\dagger M_\nu)$  in the Majorana (Dirac) neutrino case, are left invariant under the action of its Abelian subgroups  $G_e$  and  $G_\nu$ , respectively. These *residual symmetries* constrain the forms of the unitary matrices  $U_e$  and  $U_\nu$  diagonalising  $M_e M_e^\dagger$  and  $M_\nu (M_\nu^\dagger M_\nu)$ , and thus of the Pontecorvo, Maki, Nakagawa, Sakata (PMNS) neutrino mixing matrix  $U_{\text{PMNS}} = U_e^\dagger U_\nu$ .

If  $G_e = Z_k$ ,  $k > 2$  or  $Z_m \times Z_n$ ,  $m, n \geq 2$ , and  $G_\nu = Z_2 \times Z_2$  ( $G_\nu = Z_k$ ,  $k > 2$  or  $Z_m \times Z_n$ ,  $m, n \geq 2$ ) for Majorana (Dirac) neutrinos, the matrices  $U_e$  and  $U_\nu$  are fixed (up to permutations of columns and diagonal phase matrix on the right). This leads to certain fixed values of the solar, atmospheric and reactor neutrino mixing angles  $\theta_{12}$ ,  $\theta_{23}$  and  $\theta_{13}$  of the PMNS matrix<sup>3</sup>. Tri-bimaximal (TBM) mixing [15–18] (see also [19]), characterised by  $\theta_{12} = \arcsin(1/\sqrt{3}) \approx 35^\circ$ ,  $\theta_{23} = 45^\circ$  and  $\theta_{13} = 0^\circ$ , is a well-known example of a symmetry form arising from a specific breaking pattern. Namely, it can be naturally realised by breaking  $G_f = S_4$  down to  $G_e = Z_3$  and  $G_\nu = Z_2 \times Z_2$  [13]. Other widely discussed examples include bimaximal (BM) mixing<sup>4</sup> ( $\theta_{12} = \theta_{23} = 45^\circ$ ,  $\theta_{13} = 0^\circ$ ) [20–22], which can be derived from

<sup>1</sup>For description of the reference 3-neutrino mixing scheme, see, e.g., [14].

<sup>2</sup>More specifically, the charged lepton and neutrino mass matrices of the charged lepton and neutrino Majorana (Dirac) mass terms written in left-right and right-left conventions, respectively.

<sup>3</sup>Throughout this article we use the standard parametrisation of the PMNS matrix (see, e.g., [14]).

<sup>4</sup>Bimaximal mixing can also be a consequence of the conservation of the lepton charge  $L' = L_e - L_\mu - L_\tau$

$G_f = S_4$  [23–25], and golden ratio A (GRA) mixing ( $\theta_{12} = \arctan(1/r) \approx 31^\circ$ ,  $\theta_{23} = 45^\circ$  and  $\theta_{13} = 0^\circ$ ,  $r = (1 + \sqrt{5})/2$  being the golden ratio) [26, 27], which can be obtained breaking  $G_f = A_5$  to  $G_e = Z_5$  and  $G_\nu = Z_2 \times Z_2$  [28, 29]. All these highly symmetric mixing patterns, however, were ruled out once  $\theta_{13}$  was measured and found to have a non-zero value,  $\theta_{13} \cong 0.15$ . The fact that  $\theta_{13}$  turned out to have a relatively large value opened up a possibility of establishing the status of Dirac CP violation (CPV) in the lepton sector by measuring the Dirac phase  $\delta$  present in the PMNS matrix. At the same time it implied, in particular, that the TBM, BM (LC), GRA and other symmetry forms of the PMNS matrix predicting  $\theta_{13} = 0$ <sup>5</sup> have to be “perturbed”, so that  $\theta_{13}$ , as well as  $\theta_{12}$  and  $\theta_{23}$ , have values compatible with the experimentally determined values. When, for example, the requisite “perturbations” are provided by the matrix  $U_e$  and have the simple form of a  $U(2)$  transformation in a plane or a product of two  $U(2)$  transformations each in a plane, the cosine of the phase  $\delta$  was shown [34, 35] to satisfy a *sum rule* by which it is expressed in terms of the three neutrino mixing angles and an angle parameter which takes discrete values depending on the underlying symmetry form (TBM, BM (LC), GRA, GRB, HG) of the PMNS matrix. Analogous sum rule for  $\cos \delta$  arises when, e.g., the TBM symmetry form of  $U_{\text{PMNS}}$  is “perturbed” on the right by a matrix describing a  $U(2)$  transformation in the 1-3 plane [36] or 2-3 plane [37]<sup>6</sup> (see, e.g., [39] for a recent review of the discussed sum rules). The measurement of  $\theta_{13} \cong 0.15$  gave also a boost to investigating alternative flavour symmetry breaking patterns in attempt to explain the special structure of the PMNS matrix.

In [38] all symmetry breaking patterns, i.e., all possible combinations of residual symmetries, which could lead to correlations between some of the three neutrino mixing angles and/or between the neutrino mixing angles and the Dirac CPV phase  $\delta$ , were considered. Namely, (A)  $G_e = Z_2$  and  $G_\nu = Z_k$ ,  $k > 2$  or  $Z_m \times Z_n$ ,  $m, n \geq 2$ ; (B)  $G_e = Z_k$ ,  $k > 2$  or  $Z_m \times Z_n$ ,  $m, n \geq 2$  and  $G_\nu = Z_2$ ; (C)  $G_e = Z_2$  and  $G_\nu = Z_2$ ; (D)  $G_e$  is fully broken and  $G_\nu = Z_k$ ,  $k > 2$  or  $Z_m \times Z_n$ ,  $m, n \geq 2$ ; and (E)  $G_e = Z_k$ ,  $k > 2$  or  $Z_m \times Z_n$ ,  $m, n \geq 2$  and  $G_\nu$  is fully broken. For each pattern, sum rules, i.e., relations between the neutrino mixing angles and/or between the neutrino mixing angles and the Dirac CPV phase  $\delta$ , when present, were derived. Neutrino mixing sum rules can be present also in the case of pattern D (E) if due to additional assumptions (e.g., additional symmetries) the otherwise unconstrained unitary matrix  $U_e$  ( $U_\nu$ ) is constrained to have the specific form of a matrix of  $U(2)$  transformation in a plane or of the product of two  $U(2)$  transformations in two different planes [34, 35, 38, 40, 41]. Therefore, the cases of patterns D and E leading to interesting phenomenological predictions are “non-minimal” from the point of view of the symmetries employed (see, e.g., [42–47]), compared to patterns A, B and C characterised by non-trivial residual symmetries present in both charged lepton and neutrino sectors, which originate from just one non-Abelian flavour symmetry.

In the present article, we concentrate on patterns A, B and C, assuming  $G_f = A_4$  ( $T'$ ),  $S_4$  and  $A_5$ . When choosing these flavour symmetries, we are guided by minimality:  $A_4$  ( $T'$ ),  $S_4$  and  $A_5$  are among smallest (in terms of the number of elements) discrete groups admitting a 3-dimensional irreducible representation. In [38] predictions for the mixing angles and  $\cos \delta$  have been obtained in the cases of patterns A, B and C originating from  $G_f = A_4$  ( $T'$ )<sup>7</sup>,  $S_4$

(LC) [5], supplemented by  $\mu - \tau$  symmetry.

<sup>5</sup>Additional examples of symmetry forms predicting  $\theta_{13} = 0$  include the golden ratio B (GRB) form ( $\theta_{12} = \arccos(r/2) = 36^\circ$ ,  $\theta_{23} = 45^\circ$ ) [30, 31] and the hexagonal (HG) form ( $\theta_{12} = 30^\circ$ ,  $\theta_{23} = 45^\circ$ ) [32, 33].

<sup>6</sup>These two sum rules can be obtained from the general results derived in [38].

<sup>7</sup>The results obtained in [38] and in the present article for the group  $A_4$  are valid also for  $T'$ , since when

and  $A_5$ , using the best fit values of other (free) mixing angles entering into the sum rules of interest. In this work, we perform a statistical analysis of the sum rule predictions derived in [38], taking into account (i) the latest global data on the neutrino mixing parameters [49], and (ii) the prospective uncertainties in the determination of the neutrino mixing angles, which are planned to be achieved in the next generation of neutrino oscillation experiments. The results of this analysis clearly demonstrate how phenomenologically viable the considered cases, and hence the  $A_4$ ,  $S_4$  and  $A_5$  flavour symmetries, are.

The layout of the remainder of this article is as follows. In Section 2, we recall the framework and recapitulate the relevant sum rules derived in [38]. In Section 3, we give a brief description of the discrete groups  $A_4$ ,  $S_4$  and  $A_5$  emphasising the features relevant for our analysis. In Section 4, we study in detail the predictions for the neutrino mixing angles and the Dirac CPV phase. We perform a statistical analysis of the predictions for  $\sin^2 \theta_{12}$ ,  $\sin^2 \theta_{23}$  and  $\cos \delta$  taking into account first the current and then the prospective uncertainties in the determination of the mixing parameters. Finally, we summarise the obtained results and conclude in Section 5.

## 2 Residual Symmetry Patterns and Sum Rules

In this section, we briefly summarise the results for patterns A, B and C obtained in ref. [38]. We will use these results in Section 4 to perform a statistical analysis of the predictions for the mixing angles and  $\cos \delta$ .

*Pattern A:*  $G_e = Z_2$  and  $G_\nu = Z_k$ ,  $k > 2$  or  $Z_m \times Z_n$ ,  $m, n \geq 2$ . The  $Z_2$  residual symmetry in the charged lepton sector fixes the matrix  $U_e$  up to a  $U(2)$  transformation in the  $i$ - $j$  plane. This transformation can be parametrised in terms of a matrix containing one angle and three phases. Two of the three phases can be removed by a redefinition of the charged lepton fields. Therefore the three neutrino mixing angles and the Dirac phase are expressed in terms of the remaining two free parameters. As a result, correlations between the observables arise. Namely, the considered type of residual symmetries leads to sum rules for  $\sin^2 \theta_{23}$  and  $\cos \delta$ , except in one case (case A3, see further) in which  $\sin^2 \theta_{12}$  and  $\sin^2 \theta_{13}$  are predicted and  $\delta$  is not constrained.

Depending on the plane in which the  $U(2)$  transformation is performed, one has three cases. The first one, which we denote as A1, corresponds to the transformation in the 1-2 plane and leads to the following sum rules:

$$\sin^2 \theta_{23} = 1 - \frac{\cos^2 \theta_{13}^\circ \cos^2 \theta_{23}^\circ}{1 - \sin^2 \theta_{13}}, \quad (2.1)$$

$$\cos \delta = \frac{\cos^2 \theta_{13} (\sin^2 \theta_{23}^\circ - \cos^2 \theta_{12}) + \cos^2 \theta_{13}^\circ \cos^2 \theta_{23}^\circ (\cos^2 \theta_{12} - \sin^2 \theta_{12} \sin^2 \theta_{13})}{\sin 2\theta_{12} \sin \theta_{13} |\cos \theta_{13}^\circ \cos \theta_{23}^\circ| (\cos^2 \theta_{13} - \cos^2 \theta_{13}^\circ \cos^2 \theta_{23}^\circ)^{\frac{1}{2}}}, \quad (2.2)$$

where the angles  $\theta_{13}^\circ$  and  $\theta_{23}^\circ$  are fixed once the flavour symmetry group  $G_f$  and the residual symmetry subgroups  $G_e$  and  $G_\nu$  are specified. In the second case, A2, which corresponds to the free  $U(2)$  transformation in the 1-3 plane, one has different relations:

$$\sin^2 \theta_{23} = \frac{\sin^2 \theta_{23}^\circ}{1 - \sin^2 \theta_{13}}, \quad (2.3)$$

---

working with the 3-dimensional and 1-dimensional irreducible representations,  $T'$  and  $A_4$  lead to the same results [48].

$$\cos \delta = -\frac{\cos^2 \theta_{13}(\cos^2 \theta_{12}^\circ \cos^2 \theta_{23}^\circ - \cos^2 \theta_{12}) + \sin^2 \theta_{23}^\circ(\cos^2 \theta_{12} - \sin^2 \theta_{12} \sin^2 \theta_{13})}{\sin 2\theta_{12} \sin \theta_{13} |\sin \theta_{23}^\circ| (\cos^2 \theta_{13} - \sin^2 \theta_{23}^\circ)^{\frac{1}{2}}}, \quad (2.4)$$

where also the angle  $\theta_{12}^\circ$  is fixed once  $G_f$ ,  $G_e$  and  $G_\nu$  are specified. Finally, case A3 corresponding to the  $U(2)$  transformation in the 2-3 plane predicts  $\sin^2 \theta_{13} = \sin^2 \theta_{13}^\circ$  and  $\sin^2 \theta_{12} = \sin^2 \theta_{12}^\circ$ , while  $\cos \delta$  remains unconstrained.

*Pattern B:*  $G_e = Z_k$ ,  $k > 2$  or  $Z_m \times Z_n$ ,  $m, n \geq 2$  and  $G_\nu = Z_2$ . The residual  $Z_2$  symmetry determines the matrix  $U_\nu$  up to a  $U(2)$  transformation in the  $i$ - $j$  plane. For Dirac neutrinos, two of the three phases parametrising this transformation can be removed by a re-phasing of the neutrino fields. For Majorana neutrinos, this is not possible, and these two phases will contribute to the Majorana phases in the PMNS matrix. In either case, they will not enter into the expressions for the mixing angles and the Dirac phase, which depend on the remaining two free parameters (an angle and a phase). Pattern B leads to sum rules for  $\sin^2 \theta_{12}$  and  $\cos \delta$ , again except in one case (case B3, see further) in which  $\sin^2 \theta_{23}$  and  $\sin^2 \theta_{13}$  are predicted and  $\delta$  is not constrained.

Again, depending on the plain of the  $U(2)$  transformation, we have three cases. Case B1 corresponding to  $(ij) = (13)$  yields

$$\sin^2 \theta_{12} = \frac{\sin^2 \theta_{12}^\circ}{1 - \sin^2 \theta_{13}}, \quad (2.5)$$

$$\cos \delta = -\frac{\cos^2 \theta_{13}(\cos^2 \theta_{12}^\circ \cos^2 \theta_{23}^\circ - \cos^2 \theta_{23}) + \sin^2 \theta_{12}^\circ(\cos^2 \theta_{23} - \sin^2 \theta_{13} \sin^2 \theta_{23})}{\sin 2\theta_{23} \sin \theta_{13} |\sin \theta_{12}^\circ| (\cos^2 \theta_{13} - \sin^2 \theta_{12}^\circ)^{\frac{1}{2}}}, \quad (2.6)$$

where  $\theta_{12}^\circ$  and  $\theta_{23}^\circ$  are fixed once the symmetries are specified. In case B2,  $(ij) = (23)$ , the sum rules of interest read:

$$\sin^2 \theta_{12} = 1 - \frac{\cos^2 \theta_{12}^\circ \cos^2 \theta_{13}^\circ}{1 - \sin^2 \theta_{13}}, \quad (2.7)$$

$$\cos \delta = \frac{\cos^2 \theta_{13}(\sin^2 \theta_{12}^\circ - \cos^2 \theta_{23}) + \cos^2 \theta_{12}^\circ \cos^2 \theta_{13}^\circ(\cos^2 \theta_{23} - \sin^2 \theta_{13} \sin^2 \theta_{23})}{\sin 2\theta_{23} \sin \theta_{13} |\cos \theta_{12}^\circ \cos \theta_{13}^\circ| (\cos^2 \theta_{13} - \cos^2 \theta_{12}^\circ \cos^2 \theta_{13}^\circ)^{\frac{1}{2}}}. \quad (2.8)$$

At last, case B3,  $(ij) = (12)$ , leads to  $\sin^2 \theta_{13} = \sin^2 \theta_{13}^\circ$  and  $\sin^2 \theta_{23} = \sin^2 \theta_{23}^\circ$ , and no sum rule for  $\cos \delta$ .

*Pattern C:*  $G_e = Z_2$  and  $G_\nu = Z_2$ . In this case, both  $U_e$  and  $U_\nu$  are determined up to  $U(2)$  transformations in the  $i$ - $j$  and  $k$ - $l$  planes, respectively. Thus, we have four free parameters (two angles and two phases) in terms of which  $\theta_{ij}$  and  $\delta$  are expressed. However, as shown in [38], this number is reduced to three after an appropriate rearrangement of these parameters. As a consequence, a sum rule for either  $\cos \delta$  or one of  $\sin^2 \theta_{ij}$  arises.

Depending on the planes in which the free  $U(2)$  transformations are performed, we have nine possibilities. We number them as in [38], i.e., cases C1–C9. Four of them lead to sum rules for  $\cos \delta$ , which we summarise bellow.

$$\text{C1, } (ij, kl) = (12, 13): \quad \cos \delta = \frac{\sin^2 \theta_{23}^\circ - \cos^2 \theta_{12} \sin^2 \theta_{23} - \cos^2 \theta_{23} \sin^2 \theta_{12} \sin^2 \theta_{13}}{\sin \theta_{13} \sin 2\theta_{23} \sin \theta_{12} \cos \theta_{12}}, \quad (2.9)$$

$$\text{C3, } (ij, kl) = (12, 23): \quad \cos \delta = \frac{\sin^2 \theta_{12} \sin^2 \theta_{23} - \sin^2 \theta_{13}^\circ + \cos^2 \theta_{12} \cos^2 \theta_{23} \sin^2 \theta_{13}}{\sin \theta_{13} \sin 2\theta_{23} \sin \theta_{12} \cos \theta_{12}}, \quad (2.10)$$

$$\text{C4, } (ij, kl) = (13, 23): \quad \cos \delta = \frac{\sin^2 \theta_{12}^\circ - \cos^2 \theta_{23} \sin^2 \theta_{12} - \cos^2 \theta_{12} \sin^2 \theta_{13} \sin^2 \theta_{23}}{\sin \theta_{13} \sin 2\theta_{23} \sin \theta_{12} \cos \theta_{12}}, \quad (2.11)$$

$$\text{C8, } (ij, kl) = (13, 13): \quad \cos \delta = \frac{\cos^2 \theta_{12} \cos^2 \theta_{23} - \cos^2 \theta_{23}^\circ + \sin^2 \theta_{12} \sin^2 \theta_{23} \sin^2 \theta_{13}}{\sin \theta_{13} \sin 2\theta_{23} \sin \theta_{12} \cos \theta_{12}}. \quad (2.12)$$

The neutrino mixing angles in these cases can be treated as free parameters. Other two cases, C5 and C9, yield correlations between  $\sin^2 \theta_{12}$  and  $\sin^2 \theta_{13}$ . Namely,

$$\text{C5, } (ij, kl) = (23, 13): \quad \sin^2 \theta_{12} = \frac{\sin^2 \theta_{12}^\circ}{1 - \sin^2 \theta_{13}}, \quad (2.13)$$

$$\text{C9, } (ij, kl) = (23, 23): \quad \sin^2 \theta_{12} = \frac{\sin^2 \theta_{12}^\circ - \sin^2 \theta_{13}}{1 - \sin^2 \theta_{13}}. \quad (2.14)$$

In cases C2 and C7, instead, there are correlations between  $\sin^2 \theta_{23}$  and  $\sin^2 \theta_{13}$ :

$$\text{C2, } (ij, kl) = (13, 12): \quad \sin^2 \theta_{23} = \frac{\sin^2 \theta_{23}^\circ}{1 - \sin^2 \theta_{13}}, \quad (2.15)$$

$$\text{C7, } (ij, kl) = (12, 12): \quad \sin^2 \theta_{23} = \frac{\sin^2 \theta_{23}^\circ - \sin^2 \theta_{13}}{1 - \sin^2 \theta_{13}}. \quad (2.16)$$

Finally, in case C6,  $(ij, kl) = (23, 12)$ ,  $\sin^2 \theta_{13}$  is predicted to be equal to  $\sin^2 \theta_{13}^\circ$ . In cases C2, C5, C6, C7 and C9,  $\cos \delta$  remains unconstrained.

In Section 4, we will apply these sum rules to derive predictions from the  $A_4$ ,  $S_4$  and  $A_5$  flavour symmetries. We recall that the parameters  $\theta_{ij}^\circ$  are fixed once the flavour symmetry group and the residual symmetry subgroups are specified.

### 3 The $A_4$ , $S_4$ and $A_5$ Symmetries

The alternating group  $A_4$  is the group of even permutations on four objects. It is isomorphic to the group of rotational symmetries of a regular tetrahedron. All its twelve elements can be expressed in terms of two generators, usually denoted as  $S$  and  $T$ , which satisfy the following presentation rules:

$$S^2 = T^3 = (ST)^3 = E, \quad (3.1)$$

$E$  being the identity of the group.  $A_4$  possesses four irreducible representations: three 1-dimensional and one 3-dimensional. The eight Abelian subgroups of  $A_4$  amount to three  $Z_2$ , four  $Z_3$  and one Klein group  $K_4$  isomorphic to  $Z_2 \times Z_2$ . The detailed list of them can be found in [50]. All these subgroups can serve as residual symmetries of the charged lepton and neutrino mass matrices<sup>8</sup>. In the case of  $A_4$ , we have pairs  $(G_e, G_\nu) = (Z_2, Z_3)$  and  $(Z_2, Z_2 \times Z_2)$  corresponding to pattern A of residual symmetries,  $(Z_3, Z_2)$  and  $(Z_2 \times Z_2, Z_2)$  to pattern B, and  $(Z_2, Z_2)$  to pattern C.

The symmetric group  $S_4$  is the group of all permutations on four objects. It is isomorphic to the group of rotational symmetries of a cube. It contains  $A_4$  as a subgroup. The 24 elements of  $S_4$  can be generated by two transformations  $\tilde{S}$  and  $\tilde{T}$  (see, e.g., [7, 8]). However, in the context of non-Abelian discrete symmetry approach to neutrino mixing, it often proves

<sup>8</sup>We recall that in the case of Majorana neutrinos the residual symmetry  $G_\nu$  can be either  $Z_2$  or  $Z_2 \times Z_2$ .

convenient to use the three generators  $S$ ,  $T$  and  $U$ , satisfying <sup>9</sup> the following presentation rules:

$$S^2 = T^3 = U^2 = (ST)^3 = (SU)^2 = (TU)^2 = (STU)^4 = E. \quad (3.2)$$

The results from [38] we are going to use in what follows were obtained working with the three generators  $S$ ,  $T$  and  $U$  of  $S_4$ . The group admits five irreducible representations: two singlet, one doublet and two triplet. The list of 20 Abelian subgroups of  $S_4$  consists of nine  $Z_2$ , four  $Z_3$ , three  $Z_4$  and four  $Z_2 \times Z_2$  groups (see, e.g., [50]).

The alternating group  $A_5$  is the group of even permutations on five objects. It is isomorphic to the group of rotational symmetries of a regular icosahedron. Obviously,  $A_4$  is contained in  $A_5$  as a subgroup. The 60 elements of  $A_5$  can be defined in terms of two generators  $S$  and  $T$ , satisfying <sup>10</sup>

$$S^2 = T^5 = (ST)^3 = E. \quad (3.3)$$

In addition to the two 3-dimensional irreducible representations, the group possesses one singlet, one 4-dimensional and one 5-dimensional representations. In total,  $A_5$  has 36 Abelian subgroups: fifteen  $Z_2$ , ten  $Z_3$ , five  $Z_2 \times Z_2$  and six  $Z_5$ . The complete list of them can be found in [29].

In [38] all possible pairs of the Abelian subgroups of  $A_4$ ,  $S_4$  and  $A_5$  listed above, which correspond to patterns A, B and C discussed in the previous section, have been considered. Using the suitable parametrisation of the PMNS matrix in each case, we have obtained the values of the fixed parameters  $\sin^2 \theta_{ij}^\circ$  relevant for the sum rules given in eqs. (2.1)–(2.16). Finally, employing these sum rules and the best fit values of the neutrino mixing angles, we have derived predictions for  $\cos \delta$  and  $\sin^2 \theta_{ij}$ . They are summarised in Tables 9–11 in [38].

In the next section, we first update the predictions for  $\cos \delta$  and  $\sin^2 \theta_{ij}$  using the best fit values of the mixing angles obtained in the latest global analysis of neutrino oscillation data [49]. Secondly, and most importantly, we perform a statistical analysis of the sum rule predictions, taking into account (i) the latest global data on the neutrino mixing parameters [49], and (ii) the prospective uncertainties in the determination of the mixing angles, which are planned to be achieved in the next generation of neutrino oscillation experiments. As we will see, the results of our analysis clearly demonstrate how phenomenologically viable the cases under consideration are at the moment and what the perspective for testing them is.

## 4 Predictions for the Mixing Angles and the Dirac CPV Phase

Before proceeding to the numerical results, we would like to make a comment on the number of possible cases we have, since a priori this number is large, and one could be surprised by a relatively small number of *viable* cases we find and present in what follows.

Let us consider as an example  $G_f = A_4$ . First, we examine the residual symmetries  $G_e$  and  $G_\nu$ , which lead to fully specified mixing patterns. There are four such types of pairs  $(G_e, G_\nu)$ . We comment on each of them below.

- $(G_e, G_\nu) = (Z_2 \times Z_2, Z_2 \times Z_2)$ . In this case, the matrices  $U_e$  and  $U_\nu$  are the same (up to permutations of columns and diagonal phase matrices on the right). Therefore, the

<sup>9</sup>This presentation of  $S_4$  is convenient, because  $S$  and  $T$  alone generate the  $A_4$  subgroup of  $S_4$ .

<sup>10</sup>We note that the generators  $S$  and  $T$  of  $A_5$  are different from the corresponding generators of  $A_4$  and  $S_4$  denoted by the same letters.

PMNS matrix is given by the unit matrix up to permutations of rows and columns and possible Majorana phases. This case is clearly non-viable.

- $(G_e, G_\nu) = (Z_3, Z_2 \times Z_2)$ . There are four such pairs in the case of  $G_f = A_4$ . All of them are conjugate to each other. As is well known, two pairs of residual symmetries, which are conjugate to each other under an element of  $G_f$ , lead to the same PMNS matrix (see, e.g., [51, 52]). Thus, it is enough to consider only one of them. The resulting PMNS matrix is fixed up to permutations of rows and columns, but is not viable (see, e.g., [52]).
- $(G_e, G_\nu) = (Z_2 \times Z_2, Z_3)$ . Again, four possible pairs are conjugate to each other and lead to the same PMNS fixed up to permutations of rows and columns. This case is not consistent with the data either.
- $(G_e, G_\nu) = (Z_3, Z_3)$ . The 16 possible  $(Z_3^{g_e}, Z_3^{g_\nu})$  pairs,  $g_e$  and  $g_\nu$  being the generating elements of the  $Z_3^{g_e}$  and  $Z_3^{g_\nu}$  subgroups, respectively, fall into two groups. There are four pairs with  $g_e = g_\nu$  and twelve pairs with  $g_e \neq g_\nu$ . The former four are conjugate to each other and lead to the same PMNS matrix, which corresponds to the unit matrix up to permutations of rows and columns. The latter twelve are also related to each other by a similarity transformation, thus leading to the same PMNS matrix fixed, as always, up to permutations of rows and columns. This pattern is not viable as well.

Secondly, considering patterns A, B and C of the residual symmetries  $G_e$  and  $G_\nu$ , which do not lead to fully specified  $U_{\text{PMNS}}$ , we have five possibilities.

- $(G_e, G_\nu) = (Z_2, Z_2 \times Z_2)$ . There are three such pairs for  $G_f = A_4$ , all of them being conjugate to each other. Thus, it is enough to consider only one of them. However, in the case of  $A_4$ , any  $Z_2$  is a subgroup of the  $Z_2 \times Z_2$ . As shown in [38],  $(G_e, G_\nu) = (Z_2^{g_e}, Z_2^{g_\nu} \times Z_2)$  and  $(G_e, G_\nu) = (Z_2^{g_e} \times Z_2, Z_2^{g_\nu})$  with  $g_e$  and  $g_\nu$  belonging to the same  $Z_2 \times Z_2$  subgroup of  $G_f$ , lead to some entries of  $U_{\text{PMNS}}$  being zero, which is ruled out by the data [49].
- $(G_e, G_\nu) = (Z_2, Z_3)$ . One can demonstrate that the twelve possible pairs are all conjugate to each other, and thus, they predict the same PMNS matrix. The latter is defined up to a free  $U(2)$  transformation applied from the left in the  $i$ - $j$  plane (3 possibilities) as explained in Section 2, and up to permutations of columns.
- $(G_e, G_\nu) = (Z_2 \times Z_2, Z_2)$ . There are three such pairs, all of them being related to each other by a similarity transformation. The same argument as for  $(G_e, G_\nu) = (Z_2, Z_2 \times Z_2)$  works in this case. The resulting PMNS matrix is not viable, because it contains zero entries.
- $(G_e, G_\nu) = (Z_3, Z_2)$ . The twelve possible pairs are all conjugate to each other, and thus, they predict the same PMNS matrix. It is defined up to a free  $U(2)$  transformation applied from the right in the  $i$ - $j$  plane (3 possibilities) as explained in Section 2, and up to permutations of columns. As we will see, the case of the transformation in the 1-3 plane is the only case consistent with the data.
- $(G_e, G_\nu) = (Z_2, Z_2)$ . The nine possible  $(Z_2^{g_e}, Z_2^{g_\nu})$  pairs can be partitioned into two equivalent classes. The first class contains three pairs with  $g_e = g_\nu$ , which are conjugate

Parameter	Best fit	$3\sigma$ range
$\sin^2 \theta_{12}$	0.307	0.272 – 0.346
$\sin^2 \theta_{23}$ (NO)	0.538	0.418 – 0.613
$\sin^2 \theta_{23}$ (IO)	0.554	0.435 – 0.616
$\sin^2 \theta_{13}$ (NO)	0.02206	0.01981 – 0.02436
$\sin^2 \theta_{13}$ (IO)	0.02227	0.02006 – 0.02452
$\delta$ [°] (NO)	234	144 – 374
$\delta$ [°] (IO)	278	192 – 354

**Table 1:** The best fit values and  $3\sigma$  ranges of the neutrino mixing parameters obtained in the latest global analysis of neutrino oscillation data [49]. NO (IO) stands for normal (inverted) ordering of the neutrino mass spectrum.

to each other. They lead to the same PMNS matrix with zero entries (see, e.g., [38, 53]). The second class consists of six pairs with  $g_e \neq g_\nu$ , all of them being related to each other by a similarity transformation. Since  $g_e, g_\nu \in Z_2 \times Z_2 \subset A_4$ , the resulting PMNS matrix contains a zero entry in this case as well [38, 53]. Therefore, the considered pattern is not viable.

Thus, the total number of cases is 64 (up to permutations of rows and columns of the PMNS matrix). Of these only 8 lead to distinct predictions for  $U_{\text{PMNS}}$ , while only five cases a priori can be phenomenologically viable<sup>11</sup>. Similar analyses can be performed for the  $S_4$  and  $A_5$  symmetries.

In our further analysis we require that all three mixing angles lie simultaneously in their respective  $3\sigma$  ranges, and that the sum rule for  $\cos \delta$ , whenever present, leads to  $|\cos \delta| \leq 1$  (see further). Thus, the number of the remaining cases gets further reduced by these requirements.

#### 4.1 Analysis with Best Fit Values

In this subsection, we use the best fit values of the mixing angles found in the latest global analysis [49] to update the numerical predictions for  $\cos \delta$  and  $\sin^2 \theta_{ij}$  obtained in [38]. For convenience, we present the current best fit values of  $\sin^2 \theta_{ij}$  and  $\delta$  along with their respective  $3\sigma$  ranges in Table 1.

In the case of  $G_f = A_4$ , there is *only one* phenomenologically viable case. Namely, this is case B1 with  $(G_e, G_\nu) = (Z_3, Z_2)$ , which yields  $(\sin^2 \theta_{12}^\circ, \sin^2 \theta_{23}^\circ) = (1/3, 1/2)$  and corresponds to the TBM mixing matrix corrected from the right by a  $U(2)$  transformation in the 1-3 plane. Making use of eqs. (2.5) and (2.6) and the current best fit values of the mixing angles for the NO neutrino mass spectrum, we find the predictions summarised in Table 2. In the next subsections we will investigate in detail how these predictions modify, if one takes into account the uncertainties in the determination of the neutrino mixing parameters.

In the case of  $G_f = S_4$ , the number of viable cases is larger, namely, there are eight viable cases. We summarise them in Table 3. In the cases marked with an asterisk, the use of the

<sup>11</sup>By “a priori” we mean that they lead to  $U_{\text{PMNS}}$  without zero entries.

$(G_e, G_\nu)$	Case	$\sin^2 \theta_{ij}^\circ$	$\cos \delta$	$\sin^2 \theta_{ij}$
$(Z_3, Z_2)$	B1	$(\sin^2 \theta_{12}^\circ, \sin^2 \theta_{23}^\circ) = (1/3, 1/2)$	-0.353	$\sin^2 \theta_{12} = 0.341$

**Table 2:** The only viable case for  $G_f = A_4$ . The values of  $\cos \delta$  and  $\sin^2 \theta_{12}$  are obtained using the best fit values of  $\sin^2 \theta_{13}$  and  $\sin^2 \theta_{23}$  for NO.

$(G_e, G_\nu)$	Case	$\sin^2 \theta_{ij}^\circ$	$\cos \delta$	$\sin^2 \theta_{ij}$
$(Z_3, Z_2)$	B1	$(\sin^2 \theta_{12}^\circ, \sin^2 \theta_{23}^\circ) = (1/3, 1/2)$	-0.353	$\sin^2 \theta_{12} = 0.341$
	B2S <sub>4</sub>	$(\sin^2 \theta_{12}^\circ, \sin^2 \theta_{13}^\circ) = (1/6, 1/5)$	0.167	$\sin^2 \theta_{12} = 0.318$
$(Z_2, Z_2)$	C1	$\sin^2 \theta_{23}^\circ = 1/4$	-1*	not fixed
	C2S <sub>4</sub>	$\sin^2 \theta_{23}^\circ = 1/2$	not fixed	$\sin^2 \theta_{23} = 0.511$
	C3	$\sin^2 \theta_{13}^\circ = 1/4$	-1*	not fixed
	C4	$\sin^2 \theta_{12}^\circ = 1/4$	1*	not fixed
	C7S <sub>4</sub>	$\sin^2 \theta_{23}^\circ = 1/2$	not fixed	$\sin^2 \theta_{23} = 0.489$
	C8	$\sin^2 \theta_{23}^\circ = 3/4$	1*	not fixed

**Table 3:** The viable cases for  $G_f = S_4$ . The values of  $\cos \delta$  and  $\sin^2 \theta_{12}/\sin^2 \theta_{23}$  are obtained using the best fit values of the relevant (not fixed) mixing angles for NO. In the cases marked with an asterisk, physical values of  $\cos \delta$  cannot be obtained employing the best fit values of the mixing angles, but they are achievable fixing two angles to their best fit values and varying the third one in its  $3\sigma$  range.

best fit values of the mixing angles leads to unphysical values of  $\cos \delta$ , i.e.,  $|\cos \delta| > 1$ , which reflects the fact that these cases cannot provide a good description of the best fit values of all three mixing angles simultaneously. However, the physical values of  $\cos \delta$  can be obtained in these cases fixing two angles to their best fit values and varying the third one in its  $3\sigma$  range.

Finally, for  $G_f = A_5$ , requiring the compatibility with the data in the way explained above, we find 13 viable cases. They are presented in Table 4. The exact algebraic forms of the irrational values of  $\sin^2 \theta_{ij}^\circ$  in Table 4 have been found in [38]. They are related to the golden ratio  $r = (1 + \sqrt{5})/2$  as follows:  $2/(4r^2 - r) \approx 0.226$ ,  $r/(6r - 6) \approx 0.436$ ,  $1/(2 + r) \approx 0.276$ ,  $1/(4r^2) \approx 0.095$ ,  $1/(3 + 3r) \approx 0.127$ , and  $(3 - r)/4 \approx 0.345$ .

We note that case B1 is common to all the three flavour symmetry groups  $A_4$ ,  $S_4$  and  $A_5$ , while cases C1, C3, C4 and C8 are shared by  $S_4$  and  $A_5$ . Thus, we have 16 cases in total, which lead to different predictions for  $\sin^2 \theta_{12}$  or  $\sin^2 \theta_{23}$  and/or  $\cos \delta$ . As we will see in the next subsection performing a statistical analysis of these predictions, two cases, namely, C4 and B2A<sub>5</sub>II, are globally disfavoured at more than  $3\sigma$  confidence level. Thus, the total number of phenomenologically viable cases reduces to 14.

## 4.2 Statistical Analysis: Current Data

It is important to perform a statistical analysis of the predictions for the mixing parameters discussed in the previous subsection in order to have a clear picture of their compatibility with the current global neutrino oscillation data as well as to assess the prospects for their

$(G_e, G_\nu)$	Case	$\sin^2 \theta_{ij}^\circ$	$\cos \delta$	$\sin^2 \theta_{ij}$
$(Z_2, Z_3)$	A1A <sub>5</sub>	$(\sin^2 \theta_{13}^\circ, \sin^2 \theta_{23}^\circ) = (0.226, 0.436)$	0.727	$\sin^2 \theta_{23} = 0.554$
	A2A <sub>5</sub>	$(\sin^2 \theta_{12}^\circ, \sin^2 \theta_{23}^\circ) = (0.226, 0.436)$	-0.727	$\sin^2 \theta_{23} = 0.446$
$(Z_3, Z_2)$	B1	$(\sin^2 \theta_{12}^\circ, \sin^2 \theta_{23}^\circ) = (1/3, 1/2)$	-0.353	$\sin^2 \theta_{12} = 0.341$
$(Z_5, Z_2)$	B1A <sub>5</sub>	$(\sin^2 \theta_{12}^\circ, \sin^2 \theta_{23}^\circ) = (0.276, 1/2)$	-0.405	$\sin^2 \theta_{12} = 0.283$
$(Z_2 \times Z_2, Z_2)$	B2A <sub>5</sub>	$(\sin^2 \theta_{12}^\circ, \sin^2 \theta_{13}^\circ) = (0.095, 0.276)$	-0.936	$\sin^2 \theta_{12} = 0.331$
	B2A <sub>5</sub> II	$(\sin^2 \theta_{12}^\circ, \sin^2 \theta_{13}^\circ) = (1/4, 0.127)$	1*	$\sin^2 \theta_{12} = 0.331$
$(Z_2, Z_2)$	C1	$\sin^2 \theta_{23}^\circ = 1/4$	-1*	not fixed
	C3A <sub>5</sub>	$\sin^2 \theta_{13}^\circ = 0.095$	1*	not fixed
	C3	$\sin^2 \theta_{13}^\circ = 1/4$	-1*	not fixed
	C4A <sub>5</sub>	$\sin^2 \theta_{12}^\circ = 0.095$	-0.799	not fixed
	C4	$\sin^2 \theta_{12}^\circ = 1/4$	1*	not fixed
	C8	$\sin^2 \theta_{23}^\circ = 3/4$	1*	not fixed
	C9A <sub>5</sub>	$\sin^2 \theta_{12}^\circ = 0.345$	not fixed	$\sin^2 \theta_{12} = 0.331$

**Table 4:** The same as in Table 3, but for  $G_f = A_5$ .

future tests. To this aim, we will follow the method of constructing an approximate global likelihood function, which was successfully applied in [35, 40, 41] (see also [54]). We briefly describe this method below.

The NuFIT collaboration performing a global analysis of neutrino oscillation data provides one-dimensional  $\chi^2$  projections for  $\sin^2 \theta_{ij}$  and  $\delta$  [49]. We denote them as  $\chi_i^2(x_i)$ ,  $i = 1, 2, 3, 4$ , where  $x_i$  are components of  $\vec{x} = (\sin^2 \theta_{12}, \sin^2 \theta_{13}, \sin^2 \theta_{23}, \delta)$ . Using these projections, we construct an approximate global  $\chi^2$  function as

$$\chi^2(\vec{x}) = \sum_{i=1}^4 \chi_i^2(x_i). \quad (4.1)$$

For each model (B1, B2S<sub>4</sub>, C1, etc.), the “standard” mixing parameters composing vector  $\vec{x}$  are not independent, but are related to each other via sum rules. Thus, in order to obtain a one-dimensional  $\chi^2$  function for the observable  $\alpha$  of interest ( $\alpha = \sin^2 \theta_{12}$ ,  $\sin^2 \theta_{23}$  or  $\cos \delta$ ), we need to minimise the global  $\chi^2(\vec{x})$  for each value of  $\alpha$  taking into account the correlations between the mixing parameters  $x_i$  (the sum rules), i.e.,

$$\chi^2(\alpha) = \min \left[ \chi^2(\vec{x}) \Big|_{\substack{\text{sum rules} \\ \alpha = \text{const}}} \right]. \quad (4.2)$$

Finally, we define the global likelihood function as

$$L(\alpha) = \exp \left( -\frac{\chi^2(\alpha)}{2} \right). \quad (4.3)$$

*Cases predicting  $\sin^2 \theta_{12}$ .* As can be seen from Tables 2–4, there are six different cases which lead to predictions for  $\sin^2 \theta_{12}$ . Namely, they read B1, B2S<sub>4</sub>, B1A<sub>5</sub>, B2A<sub>5</sub>, B2A<sub>5</sub>II and

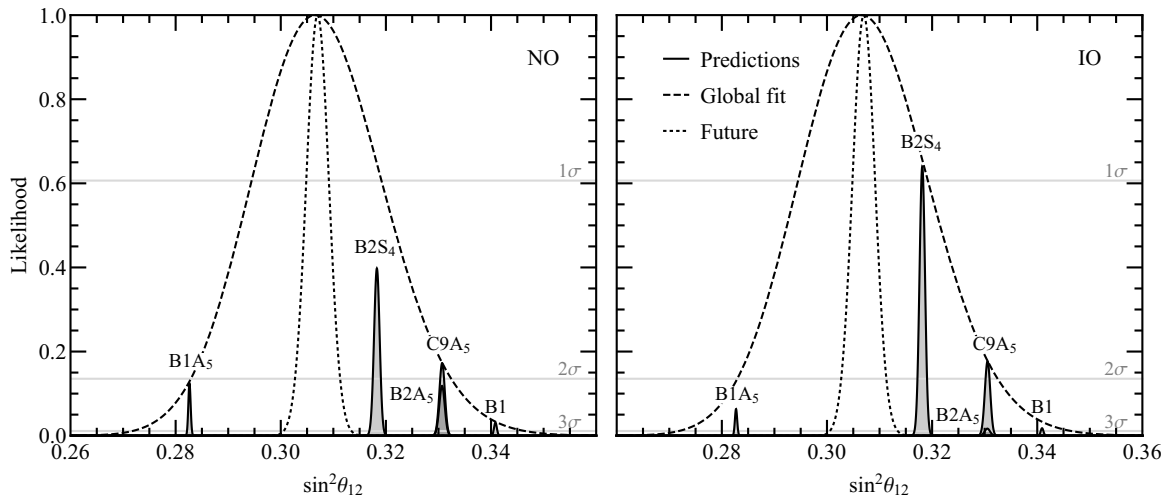


**Figure 1:** Predictions for  $\sin^2 \theta_{12}$  obtained using the current global data on the neutrino mixing parameters. “Future” (the dotted line) refers to the scenario with  $\sin^2 \theta_{12}^{\text{bf}} = 0.307$  (current best fit value) and the relative  $1\sigma$  uncertainty of 0.7% expected from the JUNO experiment. See text for further details.

C9A<sub>5</sub>. We have performed the statistical analysis of the predictions for  $\sin^2 \theta_{12}$  as described above. In Fig. 1, we present the obtained likelihood functions. In the left (right) panel, we have used as an input the one-dimensional projections  $\chi_i^2(x_i)$  for NO (IO). We would like to note that according to [49] there is an overall preference for NO over IO of  $\Delta\chi^2 = 4.14$ . However, we take a conservative approach and treat both orderings on equal grounds in our analysis.

Five cases presented in Fig. 1 lead to very sharp predictions for  $\sin^2 \theta_{12}$ . The corresponding likelihood profiles are very narrow because their widths are determined by the small uncertainty on  $\sin^2 \theta_{13}$  as can be understood from eqs. (2.5), (2.7) and (2.14). Case B1 is compatible with the global data at  $3\sigma$ . Cases B1A<sub>5</sub> and B2A<sub>5</sub> almost touch the  $2\sigma$  line for NO and are within  $3\sigma$  for IO. C9A<sub>5</sub> is compatible with the data at  $2\sigma$ . Finally, B2S<sub>4</sub> is the case which is favoured most by the present data, being compatible with them at  $1.5\sigma$  for NO and  $1\sigma$  for IO. We find that case B2A<sub>5</sub>II is globally disfavoured at more than  $3\sigma$ , the value of  $\chi^2$  in the minimum,  $\chi_{\text{min}}^2$ , being equal to 9.9 (13.7) for NO (IO). Thus, we do not present this case in Fig. 1.

The dashed line corresponds to the likelihood for  $\sin^2 \theta_{12}$  extracted from the global analysis, i.e., calculated substituting the one-dimensional projection  $\chi_1^2(\sin^2 \theta_{12})$  in eq. (4.3) in place of  $\chi^2(\alpha)$ . It is clear from the way in which the likelihood function is constructed that none of the predicted likelihood profiles can go beyond the dashed line. The dotted line instead represents the prospective precision on  $\sin^2 \theta_{12}$  of 0.7%, which is planned to be achieved by the medium-baseline reactor oscillation experiment JUNO [55]. More precisely, the corresponding likelihood is calculated using eq. (4.3) with a replacement of  $\chi^2(\alpha)$  by

$$\chi_{1,\text{future}}^2(\sin^2 \theta_{12}) = \left( \frac{\sin^2 \theta_{12} - \sin^2 \theta_{12}^{\text{bf}}}{\sigma(\sin^2 \theta_{12})} \right)^2, \quad (4.4)$$

where  $\sin^2 \theta_{12}^{\text{bf}} = 0.307$  is the current best fit value of  $\sin^2 \theta_{12}$ , and  $\sigma(\sin^2 \theta_{12}) = 0.007 \times \sin^2 \theta_{12}^{\text{bf}}$  is the prospective  $1\sigma$  uncertainty in its determination. Thus, we make an assumption that

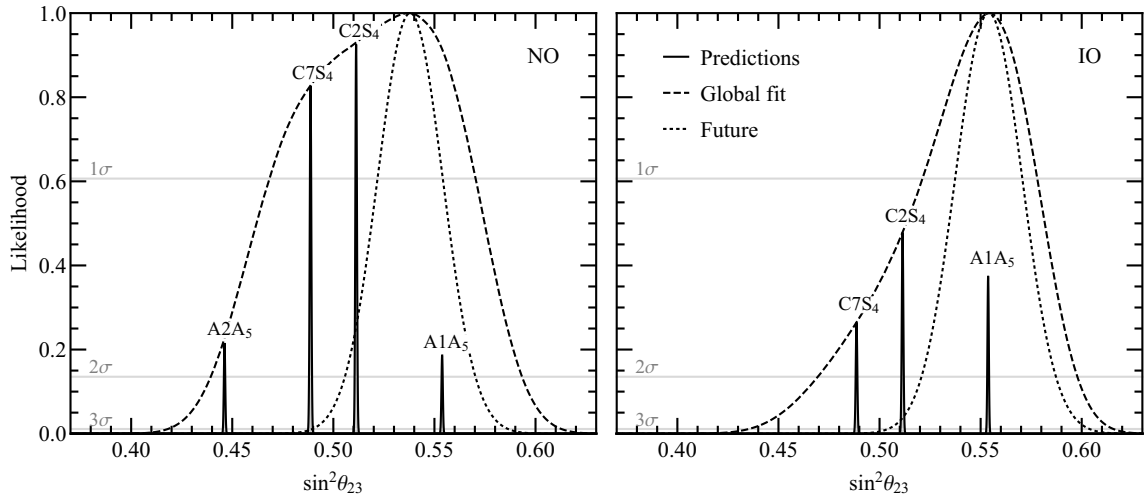


**Figure 2:** Predictions for  $\sin^2 \theta_{23}$  obtained using the current global data on the neutrino mixing parameters. “Future” (the dotted line) refers to the scenario with  $\sin^2 \theta_{23}^{\text{bf}} = 0.538$  (0.554) for NO (IO) (current best fit values) and the relative  $1\sigma$  uncertainty of 3% expected from DUNE and T2HK. See text for further details.

the best fit value of  $\sin^2 \theta_{12}$  will not change in the future. If it is indeed the case, then, as is clear from Fig. 1, all five models, B1, B2S<sub>4</sub>, B1A<sub>5</sub>, B2A<sub>5</sub> and C9A<sub>5</sub>, will be ruled out by the JUNO measurement of  $\sin^2 \theta_{12}$ . If, however, the best fit value changed coinciding, e.g., with that of case B1A<sub>5</sub> (B2S<sub>4</sub>), cases B2S<sub>4</sub> (B1A<sub>5</sub>), B2A<sub>5</sub>, C9A<sub>5</sub> and B1 would be ruled out.

*Cases predicting  $\sin^2 \theta_{23}$ .* There are four cases leading to predictions for  $\sin^2 \theta_{23}$ : C2S<sub>4</sub>, C7S<sub>4</sub>, A1A<sub>5</sub> and A2A<sub>5</sub>. We show the corresponding likelihood functions in Fig. 2. Since, in these cases  $\sin^2 \theta_{23}$  is determined by  $\sin^2 \theta_{13}$ , see eqs. (2.1), (2.3), (2.15) and (2.16), the predicted likelihood profiles are very narrow. Cases C2S<sub>4</sub> and C7S<sub>4</sub> are well compatible with the data for NO (at less than  $1\sigma$ ) and with the data for IO (at around  $1.5\sigma$ ). What concerns cases A1A<sub>5</sub> and A2A<sub>5</sub>, they reconcile with the data for NO at  $2\sigma$ . For IO, A1A<sub>5</sub> is within  $1.5\sigma$ , while A2A<sub>5</sub> is disfavoured at more than  $3\sigma$  ( $\chi_{\text{min}}^2 = 10.1$ ). This is why this case is not present in the right panel of Fig. 2.

Similarly to the previous figure, the dashed line corresponds to the global fit likelihood obtained from the one-dimensional projection  $\chi_3^2(\sin^2 \theta_{23})$ . The dotted line indicates the prospective precision on  $\sin^2 \theta_{23}$  of 3%. It is worth noting that the error on  $\sin^2 \theta_{23}$ , which can be reached in the next generation of long-baseline (LBL) neutrino oscillation experiments like DUNE [56, 57] and T2HK [58, 59], depends on the true value of this parameter. As can be seen, e.g., from Fig. 10 in [60], in the case of T2HK this error varies from 1% for the true values of  $\sin^2 \theta_{23}$  on the boundaries of its  $3\sigma$  range to approximately 6% for  $\sin^2 \theta_{23} = 0.5$ . For the current best fit value of  $\sin^2 \theta_{23} = 0.538$  (for NO), the expected uncertainty does not exceed 3%, and we take it as a benchmark value. The likelihood corresponding to the dotted line is calculated using

$$\chi_{3, \text{future}}^2(\sin^2 \theta_{23}) = \left( \frac{\sin^2 \theta_{23} - \sin^2 \theta_{23}^{\text{bf}}}{\sigma(\sin^2 \theta_{23})} \right)^2, \quad (4.5)$$

where  $\sin^2 \theta_{23}^{\text{bf}} = 0.538$  (0.554) is the current best fit value of  $\sin^2 \theta_{23}$  for NO (IO), and  $\sigma(\sin^2 \theta_{23}) = 0.03 \times \sin^2 \theta_{23}^{\text{bf}}$  is the prospective  $1\sigma$  uncertainty. If the current best fit value

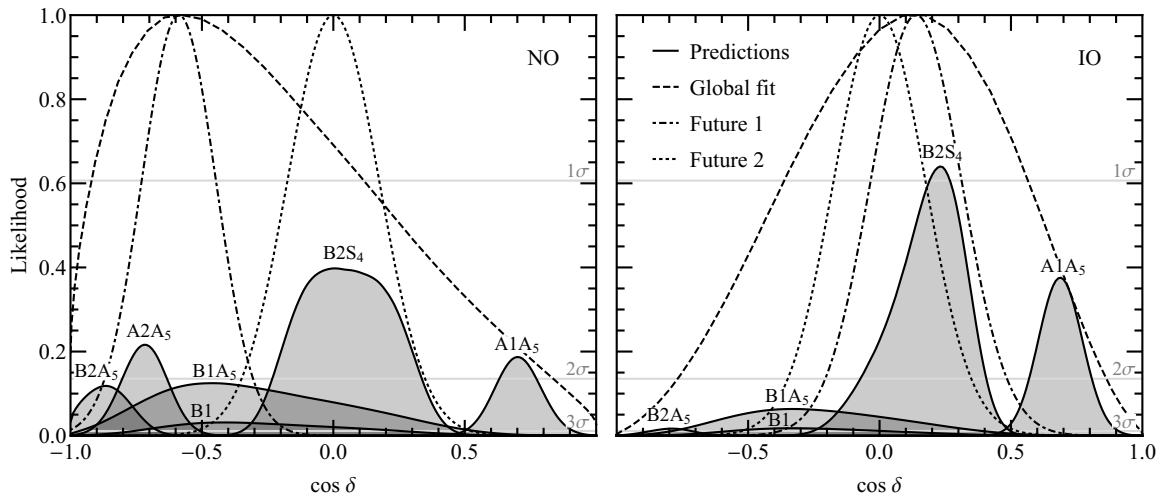


**Figure 3:** Predictions for  $\cos \delta$  in viable cases A and B obtained using the current global data on the neutrino mixing parameters. “Future 1” (the dash-dotted line) refers to the scenario with  $\delta^{\text{bf}} = 234^\circ$  ( $278^\circ$ ) for NO (IO) (current best fit values) and the  $1\sigma$  uncertainty on  $\delta$  of  $10^\circ$ . “Future 2” (the dotted line) corresponds to  $\delta^{\text{bf}} = 270^\circ$  and the  $1\sigma$  uncertainty on  $\delta$  of  $10^\circ$ . See text for further details.

does not change in the future, case  $A2A_5$  will be ruled out, while case  $C7S_4$  will be disfavoured at  $3\sigma$ . However, if the best fit value changed, e.g., to 0.5 for both NO and IO spectra, cases  $C2S_4$  and  $C7S_4$  would be phenomenologically viable, while cases  $A1A_5$  and  $A2A_5$  would be disfavoured at  $3\sigma$  (see Fig. 2).

*Cases predicting  $\cos \delta$ .* As has been discussed in Section 2 and can be seen from Tables 2–4, cases A and B of interest lead not only to predictions for  $\sin^2 \theta_{23}$  and  $\sin^2 \theta_{12}$ , respectively, but also to predictions for  $\cos \delta$ . Using eqs. (2.1)–(2.8), we have performed the statistical analysis of these predictions. The obtained results are summarised in Fig. 3. We find that the predictions for  $\cos \delta$  in cases B are very sensitive to the value of  $\theta_{23}$  (cf. eqs. (2.6) and (2.8)), which is determined with a larger uncertainty than  $\theta_{12}$  and  $\theta_{13}$ . This results in quite broad likelihood profiles. For cases A, the uncertainty in predicting  $\cos \delta$  from eqs. (2.2) and (2.4) is driven by the uncertainty on  $\sin^2 \theta_{12}$ , since  $\sin^2 \theta_{23}$  is almost fixed in these cases (see Fig. 2). Thus, the resulting likelihood profiles are not so broad in cases  $A1A_5$  and  $A2A_5$ . In each case B (A), the value of the likelihood in the maximum is the same as in Fig. 1 (Fig. 2) as should be expected from the procedure of constructing the likelihood.

The dashed line in Fig. 3 stands for the likelihood extracted from the global analysis. More precisely, we take the one-dimensional projection  $\chi_4^2(\delta)$  restricted to the interval of  $\delta \in [180^\circ, 360^\circ]$  and translate it to  $\chi_4^2(\cos \delta)$ . Then, we use the latter to construct the likelihood. At present, all values of  $\cos \delta$  are allowed at  $3\sigma$  for NO, and almost all,  $\cos \delta \in [-0.978, 0.995]$ , for IO. We also show the dash-dotted and dotted lines which represent two benchmark cases. The first case, marked in Fig. 3 as “Future 1” (the dash-dotted line), corresponds to the current best fit value  $\delta^{\text{bf}} = 234^\circ$  ( $278^\circ$ ) for NO (IO) and the prospective  $1\sigma$  uncertainty  $\sigma(\delta) = 10^\circ$ . The second case, “Future 2” (the dotted line), corresponds to the potential best fit value  $\delta^{\text{bf}} = 270^\circ$  (for both NO and IO) and the same error on  $\delta$  of  $10^\circ$ . The corresponding

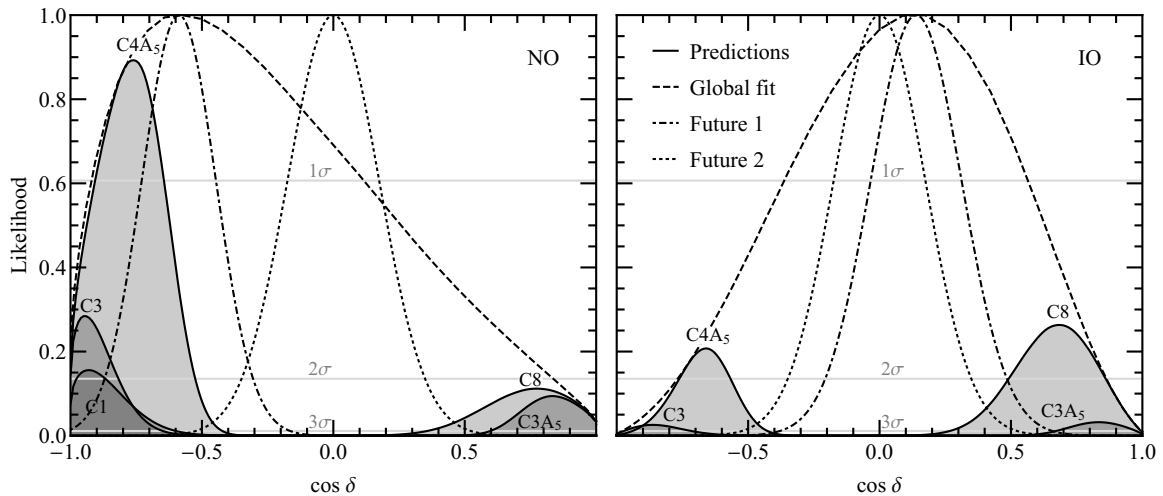


**Figure 4:** The same as in Fig. 3, but for viable cases C.

$\chi^2$  functions read

$$\chi_{4,\text{future}}^2(\cos \delta) = \left( \frac{\cos \delta - \cos \delta^{\text{bf}}}{\sigma(\cos \delta)} \right)^2, \quad (4.6)$$

where  $\sigma(\cos \delta)$  is obtained from  $\sigma(\delta) = 10^\circ$  using the derivative method of uncertainty propagation.

Finally, we perform the statistical analysis of the predictions for  $\cos \delta$  in cases C1, C3, C4, C8, C3A<sub>5</sub> and C4A<sub>5</sub>. The corresponding sum rules are given in eqs. (2.9)–(2.12). Note that none of the mixing angles are predicted in these cases. We show the obtained likelihood functions for  $\cos \delta$  in Fig. 4. As we see, all of them peak at values of  $|\cos \delta| \sim 0.5 - 1$ . There are two groups of cases: the first one consisting of C1, C3 and C4A<sub>5</sub> leads to the negative values of  $\cos \delta$ , while the second one including C8 and C3A<sub>5</sub> predicts the positive values. We find that case C4 is globally disfavoured at more than  $3\sigma$ , the corresponding  $\chi_{\text{min}}^2$  being 9.3 (13.6) for NO (IO). Therefore, we do not present this case in Fig. 4. On contrary, case C4A<sub>5</sub> is very well compatible with the data for NO, while for IO the compatibility is somewhat worse, at around  $2\sigma$ . Case C3 reconciles with the data for NO (IO) at approximately  $1.5\sigma$  ( $3\sigma$ ). Case C1, being compatible at  $2\sigma$  for NO, gets disfavoured at more than  $3\sigma$  for IO, the corresponding  $\chi_{\text{min}}^2 = 12.7$ . C8 is concordant with the data at almost  $2\sigma$  ( $1.5\sigma$ ) for NO (IO). Finally, the predictions of C3A<sub>5</sub> are compatible with the global data at  $3\sigma$ .

Looking at the dotted line, we see that if in the future the best fit value of  $\delta$  shifted to  $270^\circ$  and the LBL experiments managed to achieve the  $1\sigma$  uncertainty on  $\delta$  of  $10^\circ$ , cases C1, C3 and C3A<sub>5</sub> (C4A<sub>5</sub> and C8) would be disfavoured at more than (at around)  $3\sigma$  only by the measurement of  $\delta$ . If, however, the current best fit value of  $\delta$  for the NO spectrum is shown to be the true value for both the NO and IO spectra, cases C3A<sub>5</sub> and C8 will be ruled out by the measurement of  $\delta$  with the indicated precision. In addition, the precision on  $\sin^2 \theta_{12}$  and  $\sin^2 \theta_{23}$  will be also improved. This will modify the likelihood profiles making them narrower. In the next subsection, we will study how this improvement will affect the results presented in Figs. 1–4.

### 4.3 Statistical Analysis: Prospective Data

In this subsection, we want to assess the impact of the future precision measurements of the neutrino mixing angles on the predictions discussed in subsection 4.2. To this aim, we perform a statistical analysis of these predictions assuming that (i) the current best fit values of the mixing angles will not change in the future, and (ii) the prospective relative  $1\sigma$  uncertainties on  $\sin^2 \theta_{12}$ ,  $\sin^2 \theta_{23}$  and  $\sin^2 \theta_{13}$  will amount to 0.7%, 3% and 3%, respectively. As has already been mentioned, a measurement of  $\sin^2 \theta_{12}$  with such a high precision is expected from JUNO, while DUNE and T2HK will be able to reach 3% on  $\sin^2 \theta_{23}$  if atmospheric mixing deviates somewhat from maximal (see the discussion above eq. (4.5)). What concerns the reactor angle, Daya Bay is going to attain the precision of 3% on  $\sin^2 \theta_{13}$  by the year of 2020 [61]. The results of the analysis in this subsection should be considered only as indicative. Similar analysis should be performed when real data become available.

With these assumptions, we construct a global  $\chi_{\text{future}}^2$  function as

$$\chi^2(\vec{y}) = \sum_{i=1}^3 \chi_{i,\text{future}}^2(y_i), \quad (4.7)$$

where  $\vec{y} = (\sin^2 \theta_{12}, \sin^2 \theta_{13}, \sin^2 \theta_{23})$ , the functions  $\chi_{i,\text{future}}^2(y_i)$  with  $i = 1$  and  $i = 3$  are given in eqs. (4.4) and (4.5), respectively, and we define  $\chi_{2,\text{future}}^2(\sin^2 \theta_{13})$  as

$$\chi_{2,\text{future}}^2(\sin^2 \theta_{13}) = \left( \frac{\sin^2 \theta_{13} - \sin^2 \theta_{13}^{\text{bf}}}{\sigma(\sin^2 \theta_{13})} \right)^2, \quad (4.8)$$

with  $\sin^2 \theta_{13}^{\text{bf}} = 0.02206$  (0.02227) being the current best fit value of  $\sin^2 \theta_{13}$  for NO (IO), and  $\sigma(\sin^2 \theta_{13}) = 0.03 \times \sin^2 \theta_{13}^{\text{bf}}$  being the prospective  $1\sigma$  uncertainty in its determination. We note that by constructing  $\chi_{\text{future}}^2$  in this way, we do not assume any experimental input on  $\delta$ . We use  $\chi_{\text{future}}^2(\vec{y})$  instead of  $\chi^2(\vec{x})$  in eq. (4.2) to construct  $\chi^2(\alpha)$ . Finally, the likelihood function is calculated according to eq. (4.3).

*Cases predicting  $\sin^2 \theta_{12}$ .* As we have already mentioned earlier, it is clear from Fig. 1 that JUNO will be able to rule out all the cases predicting  $\sin^2 \theta_{12}$ , if the best fit value of this parameter does not shift in the future (see the dotted line). However, this conclusion might change if the best fit value of  $\sin^2 \theta_{12}$  changes significantly.

*Cases predicting  $\sin^2 \theta_{23}$ .* Since the predicted centre value of  $\sin^2 \theta_{23} = 0.554$  in case A1A<sub>5</sub> matches exactly the current best fit value of this parameter for IO, this case will certainly survive in the future, if  $\sin^2 \theta_{23}^{\text{bf}}$  remains the same. Moreover, the precision on  $\sin^2 \theta_{23}$  is not expected to be as high as on  $\sin^2 \theta_{12}$ , and we can infer from Fig. 2 that case C2S<sub>4</sub> has a chance to survive, while A2A<sub>5</sub> and C7S<sub>4</sub> do not. We have performed the statistical analysis with the prospective uncertainties. The obtained results presented in Fig. 5 confirm our expectations. In particular, case A1A<sub>5</sub> would be perfectly compatible with the prospective data for IO. Note that now the amplitude of the likelihood profile is maximal, since we have not assumed any information on  $\delta$ . For NO, the case under consideration would be slightly disfavoured only due to the form of  $\chi_{3,\text{future}}^2(\sin^2 \theta_{23})$  (the dotted line). C2S<sub>4</sub> would be compatible at  $2\sigma$  ( $3\sigma$ ) with the prospective data for NO (IO), which is again dictated by the dotted line. For C7S<sub>4</sub> we find  $\chi_{\text{min}}^2 = 9.3$  (15.5) for NO (IO), and thus, we do not present this case in Fig. 5. The conclusions about the excluded cases should be revised if the best fit value of  $\sin^2 \theta_{23}$  shifts, e.g., to 0.5.

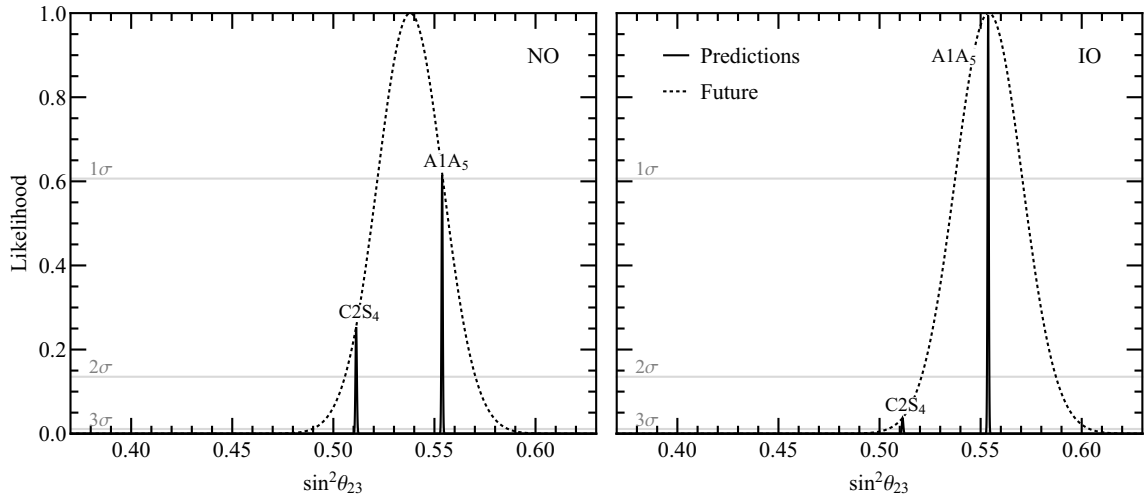


**Figure 5:** Predictions for  $\sin^2 \theta_{23}$  obtained using the current best fit values and the prospective uncertainties in the determination of the neutrino mixing angles. “Future” (the dotted line) refers to the scenario with  $\sin^2 \theta_{12}^{\text{bf}} = 0.307$  (current best fit value) and the relative  $1\sigma$  uncertainty of 0.7% expected from the JUNO experiment. See text for further details.

*Cases predicting  $\cos \delta$ .* Since all cases B as well as case A2A<sub>5</sub> would be ruled out by the prospective data we have assumed, Fig. 3 would change significantly in the future, featuring *only* case A1A<sub>5</sub>. We present the likelihoods obtained in this case for NO and IO in Fig. 6. The width of the likelihood profiles in this figure is much smaller than that of the corresponding profiles in Fig. 3. This makes even more evident the fact that improving the precision on the mixing angles leads to sharper predictions for  $\cos \delta$ , which can and should be considered as an additional motivation of measuring the mixing angles with a high precision.

Finally, we perform the statistical analysis of the predictions for  $\cos \delta$  in cases C. We show the results in Fig. 7. We find that under the assumptions made case C1 would be ruled out. Thus, we would be left with four cases. Two of them lead to predictions which are in the corners of the parameter space for  $\cos \delta$ . Namely, C3 leads to values of  $\cos \delta \lesssim -0.9$  ( $-0.8$ ) for NO (IO), while C3A<sub>5</sub> leads to  $\cos \delta \gtrsim 0.9$ . At least some of these values, if not all of them, will be ruled out by the future data on  $\delta$ . In what concerns currently viable cases C4A<sub>5</sub> and C8, they will be disfavoured at approximately  $3\sigma$  only by the measurement of  $\delta$  if the true value of  $\delta$  is indeed around  $270^\circ$  and the planned LBL experiments measure  $\delta$  with a  $1\sigma$  error of  $10^\circ$  (cf. Fig. 4). At the same time, if the current best fit value of  $\delta$  for the NO spectrum turned out to be the true value for both the NO and IO spectra, cases C3 and C4A<sub>5</sub> would “survive” this test. Thus, a high precision measurement of  $\delta$  is crucial to firmly establish the status of the considered cases.

Before concluding, let us add two comments. First, the predictions considered in the present study can be tested simulating the future neutrino oscillation experiments, as it has been recently done, e.g., in ref. [62], where DUNE and T2HK simulations have been performed to test the predictions for  $\cos \delta$  of sum rules [34] corresponding to pattern D of discrete flavour symmetry breaking (see the Introduction). We plan to present such a study elsewhere. Secondly, it has been shown in ref. [63] for the indicated set of sum rules that renormalisation group corrections to their predictions are negligible within the SM extended by the Weinberg dimension 5 operator to generate the neutrino masses, as well as in the MSSM

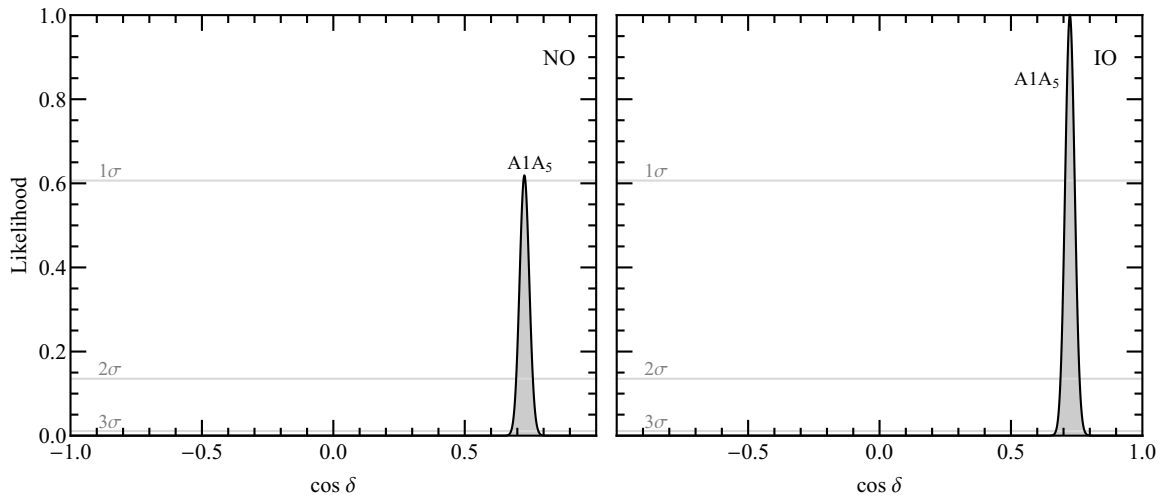


**Figure 6:** Predictions for  $\cos \delta$  in only viable case  $A1A_5$  obtained using the current best fit values and the prospective uncertainties in the determination of the neutrino mixing angles. See text for further details.

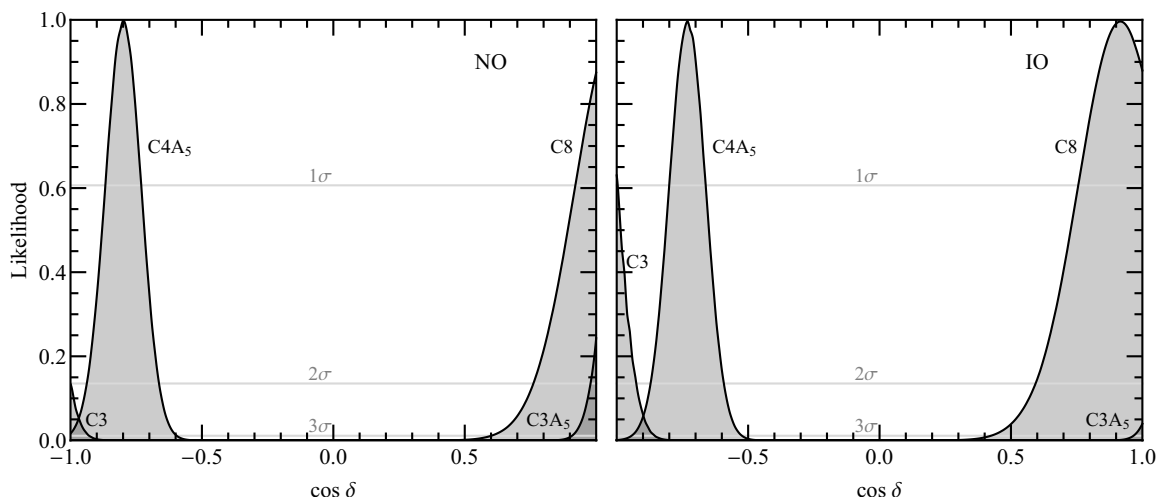


**Figure 7:** The same as in Fig. 6, but for viable cases C.

with relatively small  $\tan \beta$  and the lightest neutrino mass  $\ll 0.01$  eV. The renormalisation group corrections can be sizeable in the MSSM if these conditions are not fulfilled.

## 5 Conclusions

We have investigated the phenomenological viability of the discrete (lepton) flavour symmetries  $A_4$ ,  $S_4$  and  $A_5$  for the description of neutrino mixing. More specifically, we have considered the  $A_4$ ,  $S_4$  and  $A_5$  lepton flavour symmetry groups broken to non-trivial residual symmetry subgroups  $G_e$  and  $G_\nu$  in the charged lepton and neutrino sectors. All flavour symmetry breaking patterns considered by us involve a  $Z_2$  group as a residual symmetry in one of the two sectors, or two different  $Z_2$  groups as residual symmetries in both sectors. More

precisely, these patterns read: (A)  $G_e = Z_2$  and  $G_\nu = Z_k$ ,  $k > 2$  or  $Z_m \times Z_n$ ,  $m, n \geq 2$ ; (B)  $G_e = Z_k$ ,  $k > 2$  or  $Z_m \times Z_n$ ,  $m, n \geq 2$  and  $G_\nu = Z_2$ ; and (C)  $G_e = Z_2$  and  $G_\nu = Z_2$ . In the cases corresponding to pattern A (B) sum rules for  $\sin^2 \theta_{23}$  ( $\sin^2 \theta_{12}$ ) and  $\cos \delta$  arise, while pattern C leads to sum rules for either  $\sin^2 \theta_{12}$  or  $\sin^2 \theta_{23}$  or  $\cos \delta$  [38],  $\theta_{12}$ ,  $\theta_{23}$  and  $\delta$  being the solar, atmospheric neutrino mixing angles and the Dirac CP violation phase of the PMNS neutrino mixing matrix.

We have performed a statistical analysis of the sum rule predictions using as input the latest global neutrino oscillation data [49]. We have found 14 cases in total compatible with these data at  $3\sigma$  confidence level. Five of them lead to very sharp predictions for  $\sin^2 \theta_{12}$ , and four others to similarly sharp predictions for  $\sin^2 \theta_{23}$  (see Figs. 1 and 2). Phenomenologically viable cases A and B, which are six in total, lead as well to predictions for  $\cos \delta$  presented in Fig. 3. Five viable C cases also lead to predictions for  $\cos \delta$ , which are summarised in Fig. 4. The corresponding likelihoods peak at values of  $|\cos \delta| \sim 0.5 - 1$ . As we have shown, the number of these cases could be further reduced by a sufficiently precise measurement of  $\delta$ .

Further, we have performed a statistical analysis of the predictions discussed above assuming that (i) the current best fit values of the mixing angles will not change in the future, and (ii) the prospective relative  $1\sigma$  uncertainties on  $\sin^2 \theta_{12}$ ,  $\sin^2 \theta_{23}$  and  $\sin^2 \theta_{13}$  will amount to 0.7%, 3% and 3%, respectively. Such uncertainties are planned to be achieved by the JUNO, T2HK/DUNE and Daya Bay experiments, respectively. Under the assumptions made, all the cases predicting  $\sin^2 \theta_{12}$  (see Fig. 1) get ruled out. In what concerns the cases predicting  $\sin^2 \theta_{23}$ , two out of the four would “survive” this test (Fig. 5). We have found that only one case among six cases A and B viable at present would be compatible with the prospective data on the neutrino mixing angles. The predictions for  $\cos \delta$  in this case are shown in Fig. 6. Four out of five cases C predicting  $\cos \delta$  satisfy the expected constraints on the mixing angles. The corresponding predictions are summarised in Fig. 7. Thus, in total six cases out of 14 viable at present are compatible with the assumed prospective data on the neutrino mixing angles, provided the current best fit values of the three neutrino mixing angles will not change drastically in the future. Five of these cases will be further critically tested by sufficiently precise data on the Dirac phase  $\delta$ , e.g., if  $\delta$  is measured with  $1\sigma$  uncertainty of  $10^\circ$ . Obviously, the results obtained with the prospective data might change with the accumulation of new data if, e.g., the current best fit values of  $\sin^2 \theta_{12}$  and/or  $\sin^2 \theta_{23}$  change significantly.

In summary, we have shown that the  $A_4$ ,  $S_4$  and  $A_5$  lepton flavour symmetries, broken to non-trivial residual symmetries in the charged lepton and neutrino sectors, lead in the case of 3-neutrino mixing to a relatively small number of phenomenologically viable cases characterised by distinct predictions for the solar or atmospheric neutrino mixing angles  $\theta_{12}$  and  $\theta_{23}$  and/or for the cosine of the Dirac CP violation phase  $\delta$ . We have also shown that the high precision measurements of the three neutrino mixing angles, planned to be performed by Daya Bay and the next generation of neutrino oscillation experiments — JUNO, T2HK, DUNE — can reduce the number of the phenomenologically viable cases to six. Five of these cases will be further critically tested by sufficiently precise data on the Dirac phase  $\delta$  that could be provided by the T2HK and DUNE experiments.

The results obtained in the present study show that the future high precision data on the three neutrino mixing angles and on the leptonic Dirac CP violation phase  $\delta$ , planned to be obtained in the Daya Bay, T2K, NO $\nu$ A, and especially by the JUNO, T2HK and DUNE experiments, will be crucial for testing the ideas of existence of new fundamental underlying discrete (non-Abelian) symmetry of the PMNS neutrino mixing matrix and of the lepton sector of particle physics.

## Acknowledgements

We would like to thank I. Girardi for the enjoyable collaboration on problems related to this work. This project received funding from the European Union's Horizon 2020 research and innovation programme under the Marie Skłodowska-Curie grant agreements No 674896 (ITN Elusives) and No 690575 (RISE InvisiblesPlus). The work of S.T.P. was supported in part by the INFN program on Theoretical Astroparticle Physics (TASP) and by the World Premier International Research Center Initiative (WPI Initiative, MEXT), Japan. A.V.T. would like to thank Kavli IPMU for the hospitality and support during the final stages of the work on this project.

## References

- [1] C. D. Froggatt and H. B. Nielsen, *Hierarchy of Quark Masses, Cabibbo Angles and CP Violation*, *Nucl. Phys.* **B147** (1979) 277–298.
- [2] R. Barbieri and L. J. Hall, *A Grand unified supersymmetric theory of flavor*, *Nuovo Cim.* **A110** (1997) 1–30 [[arXiv:hep-ph/9605224](#)].
- [3] R. Barbieri, L. J. Hall, S. Raby and A. Romanino, *Unified theories with  $U(2)$  flavor symmetry*, *Nucl. Phys.* **B493** (1997) 3–26 [[arXiv:hep-ph/9610449](#)].
- [4] R. Barbieri, L. J. Hall and A. Romanino, *Consequences of a  $U(2)$  flavor symmetry*, *Phys. Lett.* **B401** (1997) 47–53 [[arXiv:hep-ph/9702315](#)].
- [5] S. T. Petcov, *On Pseudodirac Neutrinos, Neutrino Oscillations and Neutrinoless Double beta Decay*, *Phys. Lett.* **110B** (1982) 245–249.
- [6] S. F. King and G. G. Ross, *Fermion masses and mixing angles from  $SU(3)$  family symmetry and unification*, *Phys. Lett.* **B574** (2003) 239–252 [[arXiv:hep-ph/0307190](#)].
- [7] G. Altarelli and F. Feruglio, *Discrete Flavor Symmetries and Models of Neutrino Mixing*, *Rev. Mod. Phys.* **82** (2010) 2701–2729 [[arXiv:1002.0211](#)].
- [8] H. Ishimori, T. Kobayashi, H. Ohki, Y. Shimizu, H. Okada and M. Tanimoto, *Non-Abelian Discrete Symmetries in Particle Physics*, *Prog. Theor. Phys. Suppl.* **183** (2010) 1–163 [[arXiv:1003.3552](#)].
- [9] S. F. King and C. Luhn, *Neutrino Mass and Mixing with Discrete Symmetry*, *Rept. Prog. Phys.* **76** (2013) 056201 [[arXiv:1301.1340](#)].
- [10] I. Esteban, M. C. Gonzalez-Garcia, M. Maltoni, I. Martinez-Soler and T. Schwetz, *Updated fit to three neutrino mixing: exploring the accelerator-reactor complementarity*, *JHEP* **01** (2017) 087 [[arXiv:1611.01514](#)].
- [11] F. Capozzi, E. Di Valentino, E. Lisi, A. Marrone, A. Melchiorri and A. Palazzo, *Global constraints on absolute neutrino masses and their ordering*, *Phys. Rev.* **D95** (2017) 096014 [[arXiv:1703.04471](#)].
- [12] P. F. de Salas, D. V. Forero, C. A. Ternes, M. Tortola and J. W. F. Valle, *Status of neutrino oscillations 2017*, [arXiv:1708.01186](#).

- [13] C. S. Lam, *Determining Horizontal Symmetry from Neutrino Mixing*, *Phys. Rev. Lett.* **101** (2008) 121602 [[arXiv:0804.2622](#)].
- [14] K. Nakamura and S. T. Petcov, *Neutrino Mass, Mixing, and Oscillations*, in PARTICLE DATA GROUP Collaboration, C. Patrignani et al., *Review of Particle Physics*, *Chin. Phys.* **C40** (2016) 100001.
- [15] P. F. Harrison, D. H. Perkins and W. G. Scott, *Tri-bimaximal mixing and the neutrino oscillation data*, *Phys. Lett.* **B530** (2002) 167 [[arXiv:hep-ph/0202074](#)].
- [16] P. F. Harrison and W. G. Scott, *Symmetries and generalizations of tri-bimaximal neutrino mixing*, *Phys. Lett.* **B535** (2002) 163–169 [[arXiv:hep-ph/0203209](#)].
- [17] Z.-z. Xing, *Nearly tri bimaximal neutrino mixing and CP violation*, *Phys. Lett.* **B533** (2002) 85–93 [[arXiv:hep-ph/0204049](#)].
- [18] X. G. He and A. Zee, *Some simple mixing and mass matrices for neutrinos*, *Phys. Lett.* **B560** (2003) 87–90 [[arXiv:hep-ph/0301092](#)].
- [19] L. Wolfenstein, *Oscillations Among Three Neutrino Types and CP Violation*, *Phys. Rev.* **D18** (1978) 958–960.
- [20] F. Vissani, *A Study of the scenario with nearly degenerate Majorana neutrinos*, [arXiv:hep-ph/9708483](#).
- [21] V. D. Barger, S. Pakvasa, T. J. Weiler and K. Whisnant, *Bimaximal mixing of three neutrinos*, *Phys. Lett.* **B437** (1998) 107–116 [[arXiv:hep-ph/9806387](#)].
- [22] A. J. Baltz, A. S. Goldhaber and M. Goldhaber, *The Solar neutrino puzzle: An Oscillation solution with maximal neutrino mixing*, *Phys. Rev. Lett.* **81** (1998) 5730–5733 [[arXiv:hep-ph/9806540](#)].
- [23] G. Altarelli, F. Feruglio and L. Merlo, *Revisiting Bimaximal Neutrino Mixing in a Model with  $S_4$  Discrete Symmetry*, *JHEP* **05** (2009) 020 [[arXiv:0903.1940](#)].
- [24] D. Meloni, *Bimaximal mixing and large  $\theta_{13}$  in a SUSY  $SU(5)$  model based on  $S_4$* , *JHEP* **10** (2011) 010 [[arXiv:1107.0221](#)].
- [25] G.-J. Ding and Y.-L. Zhou, *Dirac Neutrinos with  $S_4$  Flavor Symmetry in Warped Extra Dimensions*, *Nucl. Phys.* **B876** (2013) 418–452 [[arXiv:1304.2645](#)].
- [26] A. Datta, F.-S. Ling and P. Ramond, *Correlated hierarchy, Dirac masses and large mixing angles*, *Nucl. Phys.* **B671** (2003) 383–400 [[arXiv:hep-ph/0306002](#)].
- [27] Y. Kajiyama, M. Raidal and A. Strumia, *The Golden ratio prediction for the solar neutrino mixing*, *Phys. Rev.* **D76** (2007) 117301 [[arXiv:0705.4559](#)].
- [28] L. L. Everett and A. J. Stuart, *Icosahedral ( $A(5)$ ) Family Symmetry and the Golden Ratio Prediction for Solar Neutrino Mixing*, *Phys. Rev.* **D79** (2009) 085005 [[arXiv:0812.1057](#)].
- [29] G.-J. Ding, L. L. Everett and A. J. Stuart, *Golden Ratio Neutrino Mixing and  $A_5$  Flavor Symmetry*, *Nucl. Phys.* **B857** (2012) 219–253 [[arXiv:1110.1688](#)].

- [30] W. Rodejohann, *Unified Parametrization for Quark and Lepton Mixing Angles*, *Phys. Lett.* **B671** (2009) 267–271 [[arXiv:0810.5239](#)].
- [31] A. Adulpravitchai, A. Blum and W. Rodejohann, *Golden Ratio Prediction for Solar Neutrino Mixing*, *New J. Phys.* **11** (2009) 063026 [[arXiv:0903.0531](#)].
- [32] C. H. Albright, A. Dueck and W. Rodejohann, *Possible Alternatives to Tri-bimaximal Mixing*, *Eur. Phys. J.* **C70** (2010) 1099–1110 [[arXiv:1004.2798](#)].
- [33] J. E. Kim and M.-S. Seo, *Quark and lepton mixing angles with a dodeca-symmetry*, *JHEP* **02** (2011) 097 [[arXiv:1005.4684](#)].
- [34] S. T. Petcov, *Predicting the values of the leptonic CP violation phases in theories with discrete flavour symmetries*, *Nucl. Phys.* **B892** (2015) 400–428 [[arXiv:1405.6006](#)].
- [35] I. Girardi, S. T. Petcov and A. V. Titov, *Predictions for the Leptonic Dirac CP Violation Phase: a Systematic Phenomenological Analysis*, *Eur. Phys. J.* **C75** (2015) 345 [[arXiv:1504.00658](#)].
- [36] W. Grimus and L. Lavoura, *A Model for trimaximal lepton mixing*, *JHEP* **09** (2008) 106 [[arXiv:0809.0226](#)].
- [37] C. H. Albright and W. Rodejohann, *Comparing Trimaximal Mixing and Its Variants with Deviations from Tri-bimaximal Mixing*, *Eur. Phys. J.* **C62** (2009) 599–608 [[arXiv:0812.0436](#)].
- [38] I. Girardi, S. T. Petcov, A. J. Stuart and A. V. Titov, *Leptonic Dirac CP Violation Predictions from Residual Discrete Symmetries*, *Nucl. Phys.* **B902** (2016) 1–57 [[arXiv:1509.02502](#)].
- [39] S. T. Petcov, *Discrete Flavour Symmetries, Neutrino Mixing and Leptonic CP Violation*, [arXiv:1711.10806](#).
- [40] D. Marzocca, S. T. Petcov, A. Romanino and M. C. Sevilla, *Nonzero  $|U_{e3}|$  from Charged Lepton Corrections and the Atmospheric Neutrino Mixing Angle*, *JHEP* **05** (2013) 073 [[arXiv:1302.0423](#)].
- [41] I. Girardi, S. T. Petcov and A. V. Titov, *Determining the Dirac CP Violation Phase in the Neutrino Mixing Matrix from Sum Rules*, *Nucl. Phys.* **B894** (2015) 733–768 [[arXiv:1410.8056](#)].
- [42] A. Meroni, S. T. Petcov and M. Spinrath, *A SUSY  $SU(5) \times T'$  Unified Model of Flavour with large  $\theta_{13}$* , *Phys. Rev.* **D86** (2012) 113003 [[arXiv:1205.5241](#)].
- [43] C. Hagedorn and D. Meloni,  *$D_{14}$  - A Common Origin of the Cabibbo Angle and the Lepton Mixing Angle  $\theta_{13}^l$* , *Nucl. Phys.* **B862** (2012) 691–709 [[arXiv:1204.0715](#)].
- [44] S. Antusch, C. Gross, V. Maurer and C. Sluka, *A flavour GUT model with  $\theta_{13}^{\text{PMNS}} \simeq \theta_C/\sqrt{2}$* , *Nucl. Phys.* **B877** (2013) 772–791 [[arXiv:1305.6612](#)].
- [45] M.-C. Chen, J. Huang, K. T. Mahanthappa and A. M. Wijangco, *Large  $\theta_{13}$  in a SUSY  $SU(5) \times T'$  Model*, *JHEP* **10** (2013) 112 [[arXiv:1307.7711](#)].

- [46] I. Girardi, A. Meroni, S. T. Petcov and M. Spinrath, *Generalised geometrical CP violation in a  $T'$  lepton flavour model*, *JHEP* **02** (2014) 050 [[arXiv:1312.1966](#)].
- [47] J. Gehrlein, J. P. Oppermann, D. Schfer and M. Spinrath, *An  $SU(5) \times A_5$  golden ratio flavour model*, *Nucl. Phys.* **B890** (2014) 539–568 [[arXiv:1410.2057](#)].
- [48] F. Feruglio, C. Hagedorn, Y. Lin and L. Merlo, *Tri-bimaximal Neutrino Mixing and Quark Masses from a Discrete Flavour Symmetry*, *Nucl. Phys.* **B775** (2007) 120–142 [Erratum: *ibid.* **B836** (2010) 127–128] [[arXiv:hep-ph/0702194](#)].
- [49] I. Esteban, M. C. Gonzalez-Garcia, A. Hernandez-Cabezudo, M. Maltoni, I. Martinez-Soler and T. Schwetz, *NuFIT 3.2: Three-neutrino fit based on data available in January 2018*, [www.nu-fit.org](#).
- [50] M. Tanimoto, *Neutrinos and flavor symmetries*, *AIP Conf. Proc.* **1666** (2015) 120002.
- [51] F. Feruglio, C. Hagedorn and R. Ziegler, *Lepton Mixing Parameters from Discrete and CP Symmetries*, *JHEP* **07** (2013) 027 [[arXiv:1211.5560](#)].
- [52] G.-J. Ding, S. F. King and A. J. Stuart, *Generalised CP and  $A_4$  Family Symmetry*, *JHEP* **12** (2013) 006 [[arXiv:1307.4212](#)].
- [53] J. T. Penedo, S. T. Petcov and A. V. Titov, *Neutrino mixing and leptonic CP violation from  $S_4$  flavour and generalised CP symmetries*, *JHEP* **12** (2017) 022 [[arXiv:1705.00309](#)].
- [54] I. Girardi, S. T. Petcov and A. V. Titov, *Predictions for the Dirac CP Violation Phase in the Neutrino Mixing Matrix*, *Int. J. Mod. Phys.* **A30** (2015) 1530035 [[arXiv:1504.02402](#)].
- [55] JUNO Collaboration, F. An et al., *Neutrino Physics with JUNO*, *J. Phys.* **G43** (2016) 030401 [[arXiv:1507.05613](#)].
- [56] DUNE Collaboration, R. Acciarri et al., *Long-Baseline Neutrino Facility (LBNF) and Deep Underground Neutrino Experiment (DUNE) Conceptual Design Report, Volume 1: The LBNF and DUNE Projects*, [arXiv:1601.05471](#).
- [57] DUNE Collaboration, R. Acciarri et al., *Long-Baseline Neutrino Facility (LBNF) and Deep Underground Neutrino Experiment (DUNE) Conceptual Design Report, Volume 2: The Physics Program for DUNE at LBNF*, [arXiv:1512.06148](#).
- [58] HYPER-KAMIOKANDE WORKING GROUP Collaboration, K. Abe et al., *A Long Baseline Neutrino Oscillation Experiment Using J-PARC Neutrino Beam and Hyper-Kamiokande*, [arXiv:1412.4673](#).
- [59] HYPER-KAMIOKANDE PROTO Collaboration, K. Abe et al., *Physics potential of a long-baseline neutrino oscillation experiment using a J-PARC neutrino beam and Hyper-Kamiokande*, *PTEP* **2015** (2015) 053C02 [[arXiv:1502.05199](#)].
- [60] P. Ballett, S. F. King, S. Pascoli, N. W. Prouse and T. Wang, *Sensitivities and synergies of DUNE and T2HK*, *Phys. Rev.* **D96** (2017) 033003 [[arXiv:1612.07275](#)].

- [61] DAYA BAY Collaboration, J. Ling, *Precision Measurement of  $\sin^2(2\theta_{13})$  and  $|\Delta m_{ee}^2|$  from Daya Bay, PoS **ICHEP2016** (2016) 467.*
- [62] S. K. Agarwalla, S. S. Chatterjee, S. T. Petcov and A. V. Titov, *Addressing Neutrino Mixing Schemes with DUNE and T2HK*, [arXiv:1711.02107](#).
- [63] J. Gehrlein, S. T. Petcov, M. Spinrath and A. V. Titov, *Renormalisation Group Corrections to Neutrino Mixing Sum Rules*, *JHEP* **11** (2016) 146 [[arXiv:1608.08409](#)].